Molecular Crystals and Liquid Crystals

Publication details, including instructions for authors and subscription information:
http://www.tandfonline.com/loi/gmcl20

Defect Mode Analysis in One-dimensional Dual Photonic Crystal with Helix

Yuko Matsuhisa [a], Yuuki Takao [a], Masanori Ozaki [a] & Ryotaro Ozaki [b]

[a] Department of Electrical, Electronic and Information Engineering, Graduate School of Engineering, Osaka University, Suita, Osaka, Japan

[b] Electrical and Electronic Engineering, National Defense Academy, Yokosuka, Japan

Version of record first published: 22 Sep 2010

To cite this article: Yuko Matsuhisa, Yuuki Takao, Masanori Ozaki & Ryotaro Ozaki (2007): Defect Mode Analysis in One-dimensional Dual Photonic Crystal with Helix, Molecular Crystals and Liquid Crystals, 478:1, 163/[919]-174/[930]

To link to this article: http://dx.doi.org/10.1080/15421400701686595

Mol. Cryst. Liq. Cryst., Vol. 478, pp. 163/[919]–174/[930], 2007

ISSN: 1542-1406 print/1563-5287 online
DOI: 10.1080/15421400701686595

Defect Mode Analysis in One-dimensional Dual Photonic Crystal with Helix

Yuko Matsuhisa
Yuuki Takao
Masanori Ozaki
Department of Electrical, Electronic and Information Engineering, Graduate School of Engineering, Osaka University, Suita, Osaka, Japan

Ryotaro Ozaki
Electrical and Electronic Engineering, National Defense Academy, Yokosuka, Japan

We have investigated optical characteristics of a one-dimensional dual photonic crystal with helix. We have confirmed the particular defect mode at the band edges of CLC has high Q-factor. The defect mode with high Q-factor existed at any conditions regardless of the polarization of incident light, helical pitch and thickness of the CLC. All defect modes in the photonic band gap could be divided in two groups. The first one was the defect modes whose Q-factor became high at the long-wavelength edge of the CLC band. The other one was that at the short-wavelength edge of the CLC.

Keywords: cholesteric liquid crystal; defect mode and dual photonic crystal

1. INTRODUCTION

A photonic crystal (PC) has a periodic dielectric structure with a periodicity in a range of optical wavelength, which has received attention as optical devices for the next generation because of the probability of controlling light. In the PC, the propagation of light is

This work is partially supported by a Grant-in-Aid for Scientific Research from the Ministry of Education, Culture, Sports, Science and Technology of Japan.

Address correspondence to Masanori Ozaki, Department of Electrical, Electronic and Information Engineering, Graduate School of Engineering, Osaka University, 2-1 Yamada-oka, Suita, Osaka 565-0871, Japan. E-mail: ozaki@opal.eei.eng.osaka-u.ac.jp

inhibited in a certain energy range of photons, which results in an appearance of a photonic band gap (PBG) [1]. Photon group velocity is suppressed at the edges of PBG. Furthermore, within a PBG, photons are localized upon the introduction of a defect in the PC [2]. By utilizing the PBG, the band edge or photon localization, various applications are expected such as low-threshold lasers, low-loss microwaveguides and so on [3–6].

Liquid crystals have been attracted attention as optical devices such as liquid crystal displays, which are attributed to optical anisotropy and response to external stress of the molecules. As other applications of LCs, PCs are also expected. Cholesteric liquid crystals (CLCs) and chiral smectic liquid crystals have chirality in the molecular structures and spontaneously form one-dimensional (1-D) periodic helical structures. If the liquid crystals have helical structures with a periodicity of optical wavelength, they can be regarded as 1-D PCs. Furthermore, in the cholesteric blue phase, three-dimensional periodic structure is spontaneously formed, which has been attracted as three-dimensional PCs. By utilizing such liquid crystals with periodic structures, various applications are expected as low-threshold lasers, tunable filters and so on [7–15].

We have so far investigated a hybrid photonic crystal which is composed of an inorganic PC and liquid crystal, and proposed a tunable PC in which PBG and defect modes can be controlled [16–23]. Recently, we have proposed a 1-D dual PC structure, which is a dielectric multilayer PC containing CLC layer as a defect and in which the defect in itself has a periodic structure due to the PC. In this configuration, we have reported the appearance of particular defect modes at photonic band edges of the CLC in the defect in addition to the defect modes for dielectric multilayer PC, and achieved low-threshold single-mode laser action based on the additional defect modes at photonic band edges of CLC [23]. However the detailed optical characteristics of the particular defect modes in the dual PC with the CLC has not been investigated. In this paper, we report the defect mode analysis of the dual PC with the CLC.

2. MODEL AND ANALYSYS METHOD

Figure 1 shows a schematic structure of a 1-D dual PC with helix in a defect, which consists of CLC and dielectric multilayers. We assumed the CLC with a right-handed helicoidal structure as an inner PC, whose helix axis is along z-axis. The thickness, helical pitch, the extraordinary and ordinary refractive indices of CLC were 9 μm, 400 nm, 1.7 and 1.5, respectively, which were general values of the CLC. The CLC

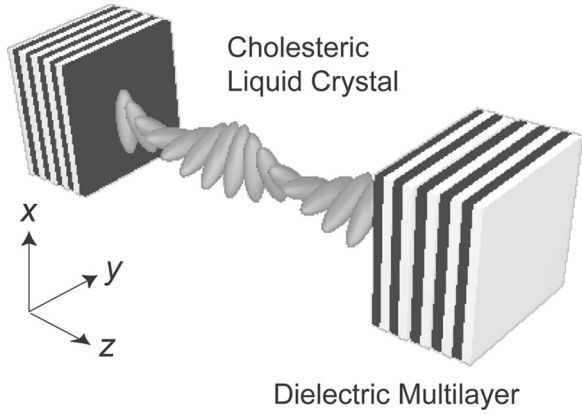

FIGURE 1 Schematic structure of 1-D dual PC with helix, which is composed with CLC sandwiched by dielectric multilayers.

was introduced between the dielectric multilayers consisting alternately stacked SiO_2 and TiO_2 layers. The total periodic number of the stack of the multilayer was ten. The refractive indices of the SiO_2 and TiO_2 were 1.46 and 2.35, and the thicknesses of them were 111 nm and 69 nm, respectively. The center wavelength of the PBG was adjusted to be 650 nm by the setting optical thickness of both SiO_2 and TiO_2 to be one-quarter of 650 nm.

In order to investigate the optical characteristics, we have performed the calculation of transmission spectrum by a method of 4×4 matrix, a numerical analysis based on Maxwell's equations, which is available in a medium varying along one direction [24]. Light propagating along the z-axis with frequency ω is given by

$$\frac{d\Psi(z)}{dz} = \frac{i\omega}{c}\mathbf{D}(z)\Psi(z), \tag{1}$$

where $\mathbf{D}(z)$ is a derivative propagation matrix and $\Psi(z) = (\mathrm{E}_x, \mathrm{H}_y, \mathrm{E}_y, \mathrm{H}_x)^{\mathrm{T}}$.

3. DEFECT MODE

Figure 2(a) shows the transmission spectra of simple CLC without any additional PCs (dashed line) and the dielectric multilayer PC (solid line). The right-handed circularly polarized light was used as incident light in this calculation. Decreasing of transmittance due to PBG for the multilayer PC appeared in the spectral range between 550 nm and 780 nm, while the PBG of the CLC was observed between 600 nm and 680 nm, and was included in that of the multilayer PC.

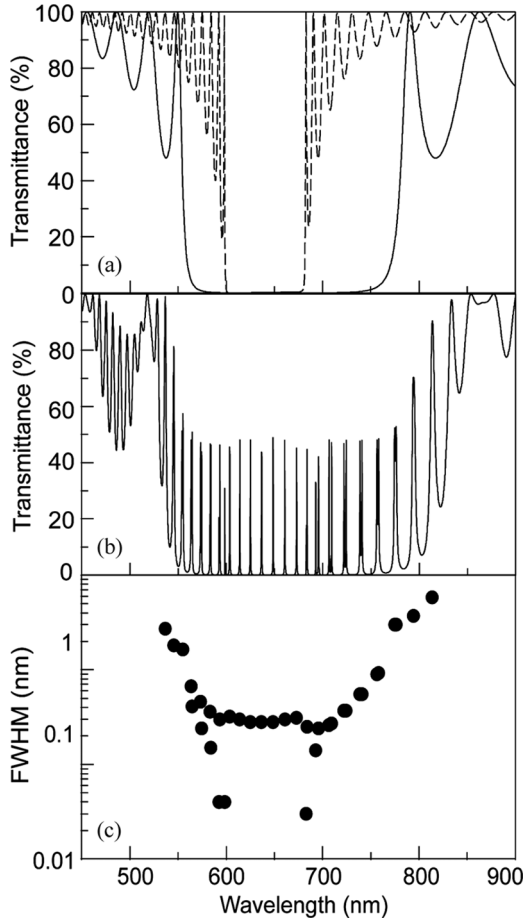

FIGURE 2 (a) Transmission spectra of a dielectric multilayer (solid line) and CLC (dashed line); (b) Transmission spectrum of a dual PC with helix consisting of dielectric multilayers and CLC shown with Figure 2(a); (c) FWHMs of defect mode peaks of a dual PC with helix.

Figure 2(b) shows the transmission spectrum of the dual PC composed of the CLC and the multilayer. The PBG was observed between 550 nm and 800 nm. Many peaks appeared in the PBG, which was due to the defect modes as a result of introduction of the CLC defect into the PC. Figure 2(c) shows the full width at half-maximum (FWHM) of each defect mode peaks in the transmission spectrum of the dual PC. The FWHM decreased gradually as closing to 650 nm which was the center wavelength of the PBG. However it dropped

drastically at 598.3 nm and 682.9 nm which correspond to the short- and long-wavelength edges of the PBG of the CLC. FWHM of these peaks were 0.02 nm which were ten times narrower than the other peaks. It should be noted that such a drastic drop of the FWHM was not observed in a 1-D PC with a uniform defect. This drop should be caused by the introduction of the CLC with a helicoidal periodic structure into the PC. From the peak width, the Q-factors of the defect modes at the band edges of the CLC were estimated to be 29900 and 34100, which were much higher than the other defect modes. The high Q-factor must be attributed to the double optical confinement effects of the CLC and the multilayer PC.

4. POLARIZATION DEPENDENCE

CLC has polarization dependence of light propagation, which results from the helicoidal structure. A circularly polarized light with the same handedness as the helix of the CLC along the helical axis reflected in the CLC defect. However the opposite-handed circularly polarized light transmits without interaction with the CLC medium. We have investigated the dependence of the transmission spectrum on incident light in a dual PC with the CLC. Figure 3 shows the transmission spectra as a function of polarization states of the incident light. The gray region shows the PBG of the CLC in the defect. Regardless of the polarization of the incident light, the PBG was observed in the spectral range between 550 nm and 800 nm, which is attributed to an isotropy of the dielectric multilayer. Many defect mode peaks were observed in all transmission spectra, which resulted from introducing the CLC defect. In the case of circularly polarized light, as shown in Figures 3(a) and (b), the transmittance of the defect modes was 50%, which is independent of the polarization of the incident light. The distribution of peak intensity of the defect modes in the PBG depends on the polarization direction of the linearly polarized light. Transmittance of defect modes decreased at the long-wavelength edge of the CLC band for linearly polarized light along x-axis as shown in Figure 3(c). In the case of 45-degree linearly polarized light, it decreased at both edges of the PBG of the CLC as shown in Figure 3(d). On the other hand, for linearly polarized light along y-axis, it decreased at the short-wavelength edge of the PBG, as shown in Figure 3(e). It should be noted that all defect modes appeared at the same wavelengths, however the transmittance at the defect modes changed as a function of the polarization of the incident light. As a calculation condition, we assumed that the CLC molecules at interfaces between the multilayer and the CLC aligned along to x-axis.

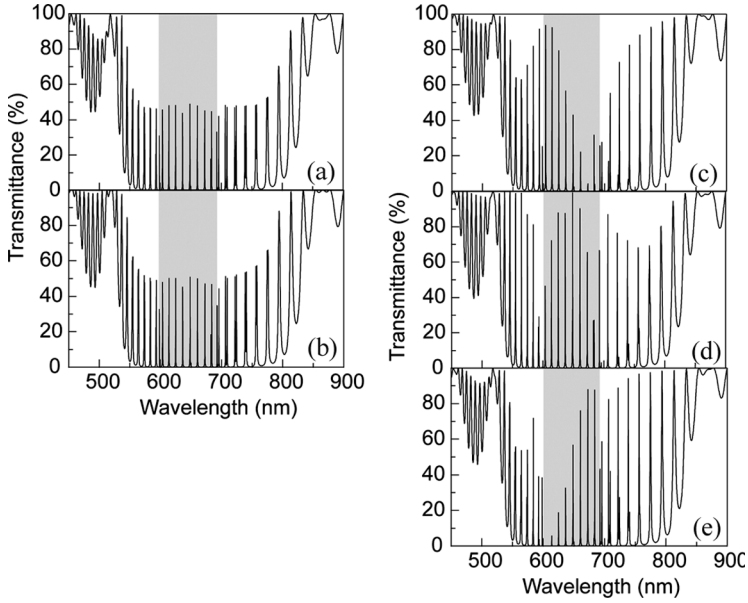

FIGURE 3 Transmission spectra of a dual PC for the incident light of various polarization state (a) and (b) are for right-handed and left-handed circularly polarized light. (c), (d) and (e) are for linearly polarized light parallel to *x*-axis, 45-degree direction, and *y*-axis, respectively.

When the *x*-axis linearly polarized light is exposed, the incident light feels extraordinary refractive index of the CLC molecules at the interface, which leads the depression of transmittance at the longer band edge of CLC. On the contrary, when the *y*-axis linearly polarized light was exposed, incident light feels ordinary refractive index at the interface, which leads to the depression of the transmittance at the short-wavelength edge of the CLC. 45-degree linearly polarized light, which is composed of *x*- and *y*-axis linearly polarized light, feels both extraordinary and ordinary refractive indices of the CLC, which makes decrease the transmittance at both long- and short-wavelength edge of the CLC. From these results, we confirmed that the polarization state of the incident light influences not to wavelength of the defect mode but to the transmittance of that. The important point to note is that the defect modes with high Q-factor necessarily appeared at the band edges of the CLC regardless of the polarization states of incident light.

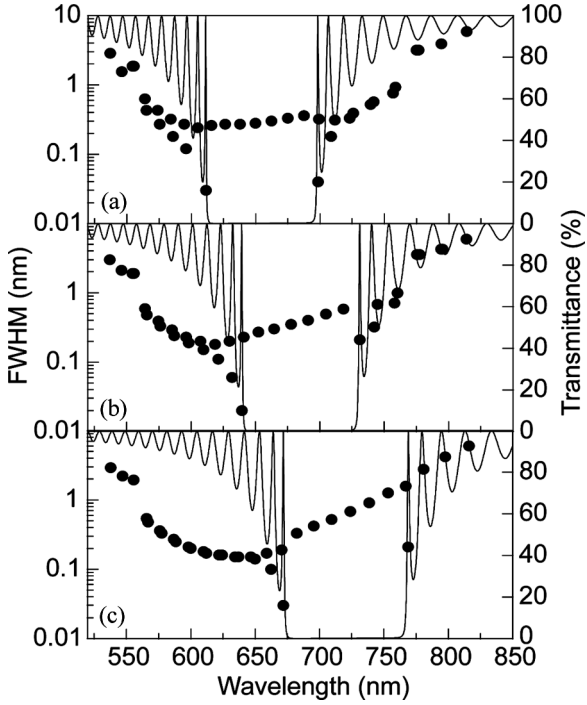

FIGURE 4 Wavelength dependence of FWHM of defect mode of a dual PC with helix (circles), and transmission spectra of CLC with the helical pitch of (a) 409.1 nm, (b) 428.6 nm and (c) 450.0 nm (dashed line).

5. HELICAL PITCH DEPENDENCE

Helical pitch of CLC can be controlled by temperature. We have investigated the helical pitch dependence of defect modes in a dual PC with helix. We assumed 9 μm as thickness of the CLC, and 409.1 nm, 428.6 nm and 450.0 nm as helical pitch of the CLC in the defect, which were set as the pitch number in the CLC defect layer would be integer. Figure 4 shows transmission spectra of simple CLC with different pitch. The PBG shifted to longer wavelength as the helical pitch elongated. Figure 4 also shows FWHM of the defect modes in the dual PC with helix. For the helical pitch of 409.1 nm, the defect modes with narrow FWHM due to high Q-factor appeared at 611.5 nm and 698.4 nm which correspond to the band edges of the CLC as shown in Figure 4(a). With elongating the helical pitch, the defect modes with narrow FWHM shifted toward longer wavelength, which is associated with the shift of the CLC band edges. From this result, we confirmed

that the defect mode with high Q-factor necessarily exists at the band edge of the CLC regardless of the helical pitch. The FWHM of the defect mode with high Q-factor minimized when the band edge of the CLC is around 650 nm which is the center wavelength of the multilayer PC band. From the result, light is strongly confined in the dual PC with helix, when the band edge of the CLC corresponds to the center wavelength of the PBG of the multilayer PC.

Figure 5 shows the wavelength of defect modes as a function of the helical pitch of the CLC in the dual PC with helix. In this calculation, we used the dual PC with the CLC defect layer of 3 μm in thickness. The wavelengths of the defect modes were almost constant on the outside of the PBG of the CLC, which was showed with the gray region. This is caused by the fact that the light out of the PBG of the CLC would not interact with the CLC medium. On the other hand, the defect modes in the PBG shifted to shorter wavelength as the helical pitch elongated, which is attributed to the interaction of the helical structure of the CLC. It should be noted that defect modes could be divided into two types. The defect modes, shown with circles in Figure 5, red-shifted at the long-wavelength edge of the CLC band as the helical pitch elongated. The other, shown with squares in Figure 5,

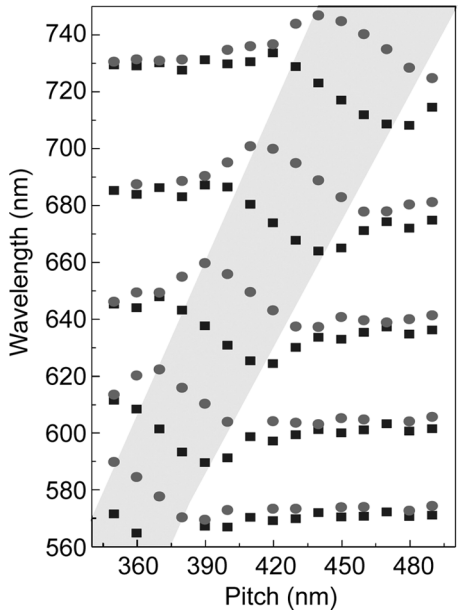

FIGURE 5 Wavelength of defect mode as a function of helical pitch of CLC.

red-shifted at the short-wavelength edge of the CLC band. From the shift and the FWHM of the defect mode, we convinced that two types of the defect modes existed in the dual PC with helix.

6. DEFECT THICKNESS DEPENDENCE

We have investigated the dependence of the defect modes wavelengths on the thickness of the CLC defect layer. Figure 6 shows the wavelength of the defect modes in the PBG as a function of thickness of the CLC. We assumed the helical pitch length of the CLC as 400 nm. The defect modes shifted to longer wavelengths as the CLC layer thickened. The defect modes can be divided into two types. One shifted gently at the short-wavelength edge of the CLC band at 590 nm as shown with circles in Figure 6, the other shown with squares shifted gently at the long-wavelength edge of the CLC band at 680 nm. The result that the defect modes can be divided into two groups supports the result shown in the previous section.

We have taken notice of one of the defect modes shown with gray circles in Figure 6. The defect mode shifted to longer wavelength as

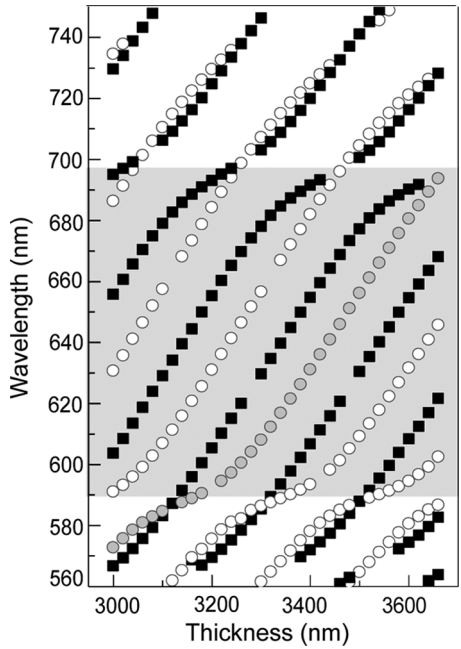

FIGURE 6 Wavelength of defect mode as a function of thickness of CLC.

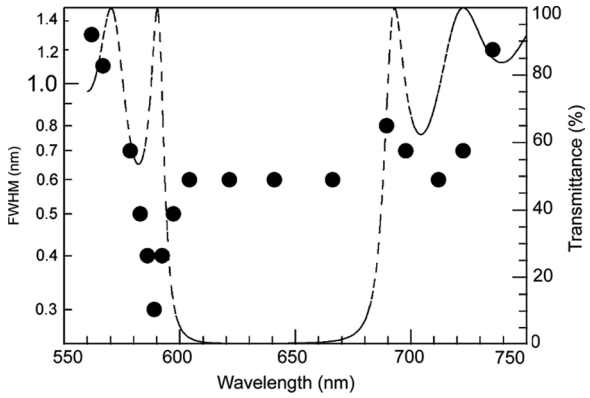

FIGURE 7 Wavelength dependence of FWHM of defect mode of a dual PC with helix (closed circles) and transmission spectrum of CLC with the thickness of 3 μm (dashed line).

the CLC layer thickened, and the shift became gentle at the short-wavelength edge of the CLC band. We have investigated FWHM of the defect modes as a function of their wavelength. The closed circles in Figure 7 show the wavelength dependence of the FWHM of the defect mode in the dual PC by changing the thickness of the CLC. We also show the transmission spectrum of the simple CLC without the multilayer PC whose thickness is assumed as 3 μm, which is shown with the dashed line in Figure 7. The FWHM increased at long and short wavelength, and drastically decreased at 589 nm which is the short-wavelength edge of the CLC band. This wavelength corresponds to the wavelength at which the defect mode gently shifted shown in Figure 6. On the other hand, a drop of the FWHM was not observed at the long-wavelength edge of the CLC band. From the result, we confirmed that the Q-factor of this defect mode became higher only at the short-wavelength edge of the CLC band. We have also investigated the Q-factor of one of the defect modes shown with squares in Figure 6, and confirmed that the defect mode showed high Q-factor only at the long-wavelength edge of the CLC band. This result denoted that two types of the defect modes exist in the dual PC with helix. One shows high Q-factor at the long-wavelength edge of the CLC band, and the other shows it at the short-wavelength edge. This phenomenon can be explained as follows. In the simple CLC without a PC, light is amplified when it localizes in the part of the high (extraordinary) refractive index at the long-wavelength band edge. In contrast,

it localizes in the part of the low (ordinary) refractive index at the short-wavelength band edge. In case of the defect mode shown in Figure 7 in the dual PC with the CLC, light tends to localize at the part of low refractive index in the CLC. It can be amplified at the short-wavelength band edge. However, at the long-wavelength band edge, the light cannot be amplified strongly because it localizes at the part of the low refractive index. Consequently, the Q-factor is enhanced only at the short-wavelength band edge of the CLC.

7. CONCLUSION

In conclusion, we investigated the optical characteristics of a dual PC with helix. The defect mode with high Q-factor was observed at the band edges of the CLC. The defect mode with high Q-factor existed at any conditions regardless of the polarization of incident light, helical pitch and thickness of the CLC. The defect modes could be divided in two groups, which interacted with long- or short-wavelength edge of the CLC band.

REFERENCES

[1] Yablonovitch, E. (1987). *Phys. Rev. Lett.*, *58*, 2059.
[2] John, S. (1987). *Phys. Rev. Lett.*, *58*, 2486.
[3] Foresi, J. S., Villeneuve, P. R., Ferrera, J., Thoen, E. R., Steinmeyer, G., Fan, S., Joannopoulos, J. D., Kimerling, L. C., Smith, H. I., Ippen, E. P. (1997). *Nature*, *390*, 143.
[4] Painter, O., Lee, R. K., Scherer, A., Yariv, A., O'Brien, J. D., Dapkus, P. D., Kim, I. (1999). *Science*, *284*, 1819.
[5] Noda, S., Chutinan, A., & Imada, M. (2000). *Nature*, *407*, 608.
[6] Hattori, T., Tsurumachi, N., & Nakatsuka, H. (1997). *J. Opt. Soc. Sm.*, *14*, 348.
[7] Ho, K. M., Chan, C. T., & Soukoulis, C. M. (1990). *Phys. Rev. Letter.*, *65*, 3152.
[8] Kopp, V. I., Fan, B., Vithana, H. K. M., & Genack, A. Z. (1998). *Opt. Lett.*, *23*, 1707.
[9] Taheri, B., Munoz, A. F., Palffy-Muhoray, P., & Twieg, R. (2001). *Mol. Cryst. Liq. Cryt.*, *358*, 73.
[10] Munoz, A. F., Palffy-Muhoray, P., & Taheri, B. (2001). *Opt. Lett.*, *26*, 804.
[11] Matsui, T., Ozaki, R., Funamoto, K., Ozaki, M., & Yoshino, K. (2002). *Appl. Phys. Lett.*, *81*, 3741.
[12] Funamoto, K., Ozaki, M., & Yoshino, K. (2003). *Jpn. J. Appl. Phys.*, *42*, L1523.
[13] Kopp, V. I., Zhang, Z., & Genack, A. Z. (2003). *Progress in Quantum Electronics*, *27*, 369.
[14] Cao, W., Munoz, A., Palffy-Muhoray, P., & Taheri, B. (2002). *Nature Materials*, *1*, 111.
[15] Ozaki, M., Ozaki, R., Matsui, T., & Yoshino, K. (2003). *Jpn. J. Appl. Phys.*, *42*, L472.
[16] Yoshino, K., Satoh, S., Shimoda, Y., Kawagishi, Y., Nakayama, K., & Ozaki, M. (1999). *Jpn. J. Appl. Phys.*, *38*, 961.
[17] Yoshino, K., Shimoda, Y., Kawagishi, Y., Nakayama, K., & Ozaki, M. (1999). *Appl. Phys. Lett.*, *75*, 932.

[18] Shimoda, Y., Ozaki, M., & Yoshino, K. (2001). *Appl. Phys. Lett.*, *79*, 3627.
[19] Ozaki, R., Matsui, T., Ozaki, M., & Yoshino, K. (2002). *Jpn. J. Appl. Phys.*, *41*, L1482.
[20] Ozaki, R., Matsui, T., Ozaki, M., & Yoshino, K. (2003). *Appl. Phys. Lett.*, *82*, 3593.
[21] Ozaki, R., Ozaki, M., & Yoshino, K. *Jpn. J. Appl. Phys.*, *42*, L669.
[22] Ozaki, R., Matsuhisa, Y., Ozaki, M., & Yoshino, K. (2004). *Appl. Phys. Lett.*, *84*, 1844.
[23] Matsuhisa, Y., Ozaki, R., Ozaki, M., & Yoshino, K. (2005). *Jpn. J. Appl. Phys.*, *44*, L629.
[24] Berreman, D. W. (1973). *J. Opt. Soc. Am.*, *63*, 1374.